

Transport properties and anisotropy of $\text{Rb}_{0.8}\text{Fe}_2\text{Se}_2$ single crystals

Chun-Hong Li¹, Bing Shen¹, Fei Han¹, Xiyu Zhu¹, and Hai-Hu Wen^{1,2}

¹ National Laboratory for Superconductivity, Institute of Physics
and Beijing National Laboratory for Condensed Matter Physics,
Chinese Academy of Sciences, P.O.Box 603, Beijing 100190, China and

² National Laboratory of Solid State Microstructures and Department of Physics, Nanjing University, Nanjing 210093, China

Single crystals of $\text{Rb}_{0.8}\text{Fe}_2\text{Se}_2$ are successfully synthesized with the superconducting transition temperatures $T_c^{\text{onset}} = 31$ K and $T_c^{\text{zero}} = 28$ K. A clear anomaly of resistivity was observed in the normal state at about 150 K, as found in a similar system $\text{K}_x\text{Fe}_2\text{Se}_2$. The upper critical field has been determined with the magnetic field along ab-plane and c-axis, yielding an anisotropy of about 3.5. The angle dependent resistivity measured below T_c allow a perfect scaling feature based on the anisotropic Ginzburg-Landau theory, leading to a consistent value of the anisotropy which decreases from about 3.6 at around T_c to 2.9 at 27 K. Comparing to the anisotropy determined for $\text{Ba}_{0.6}\text{K}_{0.4}\text{Fe}_2\text{As}_2$ and $\text{BaFe}_{1.92}\text{Co}_{0.08}\text{As}_2$ using the same method, we find that the present sample is more anisotropic and the Fermi surfaces with stronger two dimensional characters are expected.

PACS numbers: 74.25.Fy, 74.25.Op, 74.70.-b

Iron pnictide superconductors have received tremendous attention in last two years since Kamihara et al. reported superconductivity at 26 K in $\text{LaFeAsO}_{1-x}\text{F}_x$.¹ The family of the FeAs-based superconductors has been expanded rapidly. A typical example is the $(\text{Ba,Sr})\text{Fe}_2\text{As}_2$ (denoted as FeAs-122) system: the anti-ferromagnetic order is suppressed and superconductivity is induced by either K doping in the Ba or Sr sites,²⁻⁴ or Co and Ni doping in the Fe sites.^{5,6} On the other hand, superconductivity was also found in the FeAs-based parent phase LiFeAs (denoted as FeAs-111)⁷⁻⁹ and $\text{Sr}_2\text{VO}_3\text{FeAs}$ (denoted as FeAs-21311).¹⁰ Compared to these iron pnictides, FeSe has a more simple structure of only FeSe layers and no toxic arsenide,¹¹ which shows superconductivity at 8 K at ambient pressure and the transition temperature can be increased dramatically to 37 K under a high pressure.¹² Moreover, recent report showed that superconducting and magnetic properties of $\text{Fe}_y\text{Se}_x\text{Te}_{1-x}$ not only depend on the concentration ratio of Se/Te, but also strongly depend on the interstitial Fe content.¹³ Additionally, angle resolved photoemission spectroscopy (ARPES) showed that the normal state of $\text{FeSe}_{0.42}\text{Te}_{0.58}$ is a strongly correlated metal, which is significantly different from the FeAs-1111 and FeAs-122 systems.¹⁴ Therefore, the FeSe-layered materials deserve intensive studies for both fundamental physics and potential applications.

Very recently, superconductivity at around 30 K was reported in $\text{K}_x\text{Fe}_2\text{Se}_2$ (denoted as FeSe-122)¹⁵, where the potassium ions could be intercalated into the Fe_2Se_2 layers. This discovery was quickly repeated by other groups with the nominal composition $\text{K}_{0.8}\text{Fe}_2\text{Se}_2$.¹⁶ Introducing potassium into the system makes the structure change from 11-type (P4/nmm) to 122-type (I4/mmm). Up to now, the system FeSe-122 gives the highest T_c among the FeSe-layered compounds under ambient pressure. Shortly after that, Krzton-Maziopa et al. reported the crystal growth of an analog compound $\text{Cs}_{0.8}(\text{FeSe}_{0.98})_2$.¹⁷ Furthermore Fang et al.¹⁸ synthesized the systematically

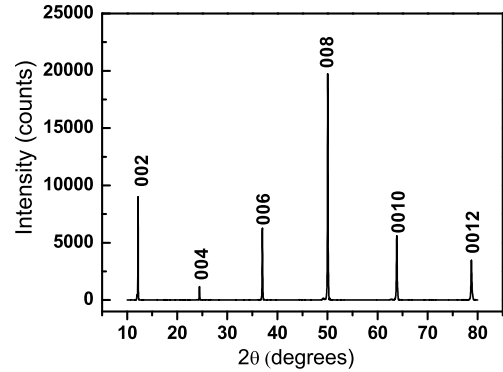


FIG. 1: (Color online) The X-ray diffraction pattern of $\text{Rb}_{0.8}\text{Fe}_2\text{Se}_2$ crystal indicates that the $(00l)$ ($l=2n$) reflections dominate the pattern.

doped $\text{K}_x\text{Fe}_2\text{Se}_2$ and found that the superconductivity might be in proximity of a Mott insulator. If just counting on the electron numbers, one would assume that $\text{A}_x\text{Fe}_2\text{Se}_2$ ($\text{A} = \text{alkaline metals}$) might be a purely electron doped sample. Thus it is curious to know whether the Fermi surfaces are close to or far different from their relatives $\text{Ba}(\text{Sr})\text{Fe}_2\text{As}_2$. The anisotropy is one of the important parameters that characterize the electronic properties. In this work, we report the successful synthesis of a new compound $\text{Rb}_{0.8}\text{Fe}_2\text{Se}_2$. The onset and zero-resistivity transition temperature were estimated to be 31 K and 28 K, respectively. We also present the temperature, magnetic field and angle dependence of resistivity. Our results point to a higher anisotropy in $\text{Rb}_x\text{Fe}_2\text{As}_2$ comparing to electron and hole doped $\text{Ba}(\text{Sr})\text{Fe}_2\text{As}_2$.

Single crystals were grown from the melt of the mixture of $\text{Rb}_{0.8}\text{Fe}_2\text{Se}_2$ using the Bridgeman method. First, FeSe powders were prepared with high-purity powder of

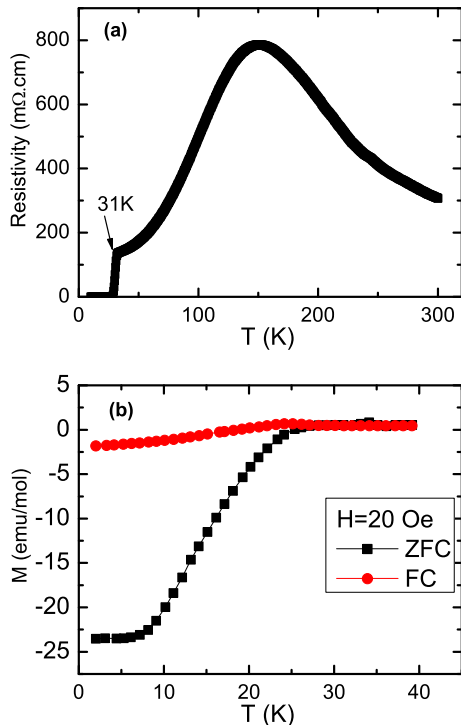


FIG. 2: (Color online) (a) Temperature dependence of resistivity for the $\text{Rb}_{0.8}\text{Fe}_2\text{Se}_2$ crystal at zero field up to 300 K. A hump of resistivity in the normal state at around 150 K can be clearly seen. (b) Temperature dependence of dc magnetization for both zero field cooling (ZFC) and field cooling processes (FC) at a magnetic field of $H = 20$ Oe.

selenium (Alfa, 99.99%) and iron (Alfa, 99.9%) by a similar method described in ref.¹⁹ Then, FeSe and Rb (Alfa, 99.75%) were mixed in appropriate stoichiometry and were put into alumina crucibles and sealed in evacuated silica ampoule. The mixture was heated up to 1030 °C and kept over 3 hours. Afterwards the melt was cooled down to 730 °C with the cooling rate of 6 °C/h and finally the furnace was cooled to room temperature with the power shut off. Well formed black crystal rods were obtained which could be easily cleaved into plates with flat shiny surfaces. The good c -axis orientation of the crystals has been demonstrated by the X-ray diffraction (XRD) analysis which show only the sharp $(00l)$ peaks. The dc magnetization measurements were done with a superconducting quantum interference device (Quantum Design, SQUID, MPMS7). The electrical transport data were collected on the Quantum Design instrument physical property measurement system (PPMS) with magnetic fields up to 9 T. The temperature stabilization was better than 0.1% and the resolution of the voltmeter was better than 10 nV. The electric contacts were made using silver paste with the contacting resistance below 0.06 Ω at room temperature.

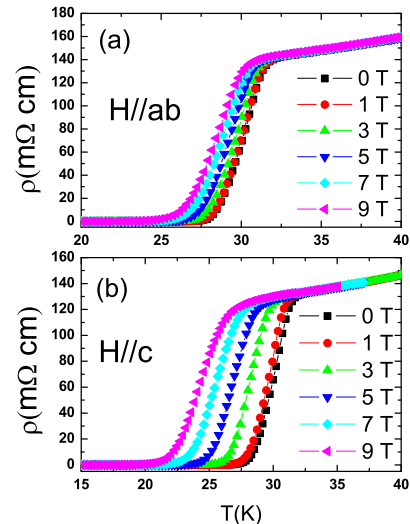


FIG. 3: (Color online) The temperature dependence of resistivity for the $\text{Rb}_{0.8}\text{Fe}_2\text{Se}_2$ single crystal at zero field and under magnetic fields of $H//ab$ (a) and $H//c$ (b) up to 9 T with increments of 2T.

Fig.2 (a) shows the temperature dependence of resistivity for a single crystal of $\text{Rb}_{0.8}\text{Fe}_2\text{Se}_2$. A superconducting transition appears at the temperature of 31 K (onset) which is similar to that of $\text{K}_{0.8}\text{Fe}_2\text{Se}_2$.¹⁵ The bulk superconductivity of our sample is also confirmed by DC magnetization measurement which is shown in Fig.2 (b), diamagnetism is clearly observed in both zero-field-cooling and field-cooling measurement. The relatively broad magnetic transition suggest that the sample is still inhomogeneous with probably the Rb distributed non-uniformly. The normal state resistivity of our sample exhibits a possible semiconductor-to-metal like transition at around 150 K. The similar behavior was also observed in $\text{K}_{0.8}\text{Fe}_2\text{Se}_2$ although in a different temperature region (about 110 K in $\text{K}_{0.8}\text{Fe}_2\text{Se}_2$). This resistivity anomaly could also possibly be caused by a structure or magnetic phase transition which is very typical in the AFe_2Se_2 superconductors. Further experiments need to be done to clarify the origin of this transition. It also should be noticed that the absolute value of normal state resistivity is quite large. The maximum value exceeds 700 $m\Omega\text{cm}$, which is hundreds of times larger than that in other typical iron-based superconductors. This phenomena could be attributed to the semiconductor background in these iron selenide superconductors.

The temperature dependence of resistivity from 15 K to 40 K with different magnetic fields applied along ab -plane or c -axis are presented in Fig. 3 (a) and (b). We adopt a criterion of $90\%\rho_n(T)$ to determine the upper critical fields. The upper critical fields of $\text{Rb}_{0.8}\text{Fe}_2\text{Se}_2$ are determined in this way and shown in Figure 4. The upper critical fields H_{c2} exhibit a rather linear temper-

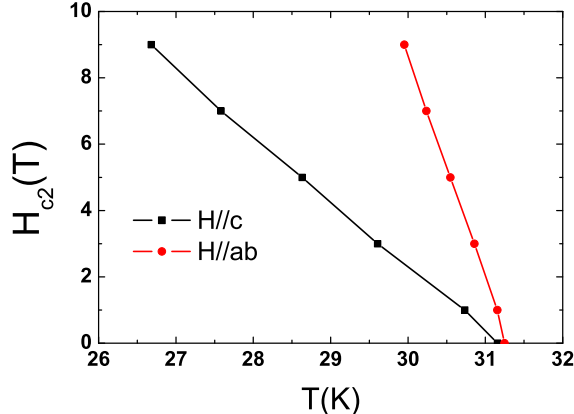


FIG. 4: (Color online) The upper critical fields of $\text{Rb}_{0.8}\text{Fe}_2\text{Se}_2$ single crystal for $H//c$ and $H//ab$ respectively.

ature dependence for both orientations. Thus we can easily get the values of the slope for two different directions of applying fields: $-dH_{c2}^{ab}/dT|_{T_c} = 6.78 \text{ T / K}$, $-dH_{c2}^c/dT|_{T_c} = 1.98 \text{ T / K}$. The former significantly exceeds the Pauli limit 1.84 T / K , which may manifest an unconventional mechanism of superconductivity in this material. With the Werthamer-Helfand-Hohenberg formula $H_{c2}(0) = -0.69 \times dH_{c2}/dT|_{T_c} T_c^{20}$ and taking $T_c = 31 \text{ K}$, we can estimate the values of upper critical fields close to zero temperature limit: $H_{c2}^{ab}(0) = 145 \text{ T}$, $H_{c2}^c(0) = 42 \text{ T}$. According Lawrence-Doniach model,²¹ the relation between the anisotropy Γ and the upper critical field are given by

$$\Gamma = (m_c/m_{ab})^{1/2} = \xi_{ab}/\xi_c = H_{c2}^{ab}/H_{c2}^c, \quad (1)$$

where H_{c2}^{ab} and H_{c2}^c are the upper critical fields with $H \parallel ab$ plane and $H \parallel c$ axis, m_c and m_{ab} are the effective masses when the electrons move along c -axis and ab -plane, ξ_{ab} and ξ_c are coherence length in ab -plane and along c -axis respectively. From the above data, we can get the anisotropy of upper critical fields of $\text{Rb}_{0.8}\text{Fe}_2\text{Se}_2$, $\Gamma \approx 3.5$. The anisotropy value is close to that in $\text{K}_{0.8}\text{Fe}_2\text{Se}_2$ ($\Gamma \approx 3.6$).¹⁶ Compared to the anisotropy in other FeAs-based superconductors, such as 5 in $\text{NdFeAsO}_{1-x}\text{F}_x$, 2-2.5 in $\text{Ba}_{1-x}\text{K}_x\text{Fe}_2\text{As}_2$, these values are all quite small compared to High- T_c cuprates, which indicates an encouraging application perspective.

Considering the uncertainties in determining the upper critical field in different formulas and by different criterion, the anisotropy ratio may subject to a modification. One major concern was that the zero temperature value $H_{c2}(0)$ was determined by using the experimental data near T_c , this concern can be removed by the measurements of angular dependent resistivity. According to the anisotropic Ginzburg-Landau theory, the effective upper

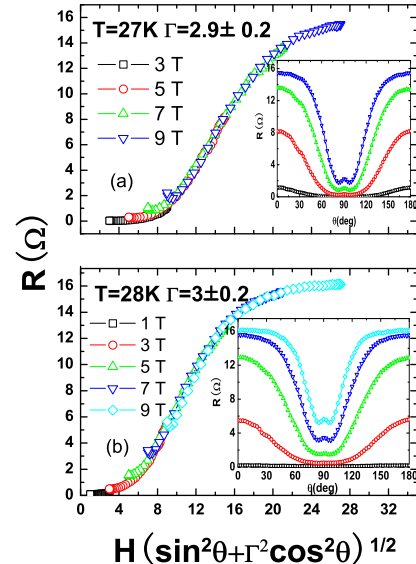


FIG. 5: Scaling of the resistivity versus $\tilde{H} = H\sqrt{\sin^2(\theta) + \Gamma^2 \cos^2(\theta)}$ at 27, 28, 29, 30 K in different magnetic fields. The curves measured at the same temperature but different magnetic fields are scaled nicely by adjusting the value of Γ . The inset presents the angular dependence of resistance for the $\text{Rb}_{0.8}\text{Fe}_2\text{Se}_2$ single crystal.

critical field $H_{c2}^{GL}(\theta)$ at an angle θ is given by

$$H_{c2}^{GL}(\theta) = H_{c2}^{ab} / \sqrt{\sin^2(\theta) + \Gamma^2 \cos^2(\theta)}. \quad (2)$$

The resistivity at different magnetic fields but a fixed temperature can be scaled with the variable $H/H_{c2}^{GL}(\theta)$. Thus by adjusting Γ , the proper scaling variable $\tilde{H} = H\sqrt{\sin^2(\theta) + \Gamma^2 \cos^2(\theta)}$ is acquired, and then the resistivity measured at different magnetic fields should collapse onto one curve²². Figure 5 presents the data of angular dependence of resistivity at 27 K, 28 K for the $\text{Rb}_{0.8}\text{Fe}_2\text{Se}_2$ single crystal. At each temperature, a cup-shaped feature centered around $\theta = 90^\circ$ is observed. The curves measured at different magnetic fields but at a fixed temperature are scaled nicely by adjusting Γ . In this treatment only one fitting parameter Γ is employed in the scaling for each temperature, so the value of Γ is more reliable than the one determined from the ratio of H_{c2}^{ab} and H_{c2}^c , which may be affected by using different criterion. At 27 K and 28 K the anisotropy Γ are found to be 2.9 ± 0.2 and 3 ± 0.2 , respectively. The results agree very well with the value determined by the ratio of H_{c2}^{ab} and H_{c2}^c , which implies the validity of the values determined in this work. In the same way, the Γ obtained at 29 K and 30 K are 3.3 ± 0.2 and 3.6 ± 0.2 , which are a little larger than those at 27 K and 28 K.

The anisotropy determined by anisotropic Ginzburg-Landau theory at different temperature of $\text{Rb}_{0.8}\text{Fe}_2\text{Se}_2$,

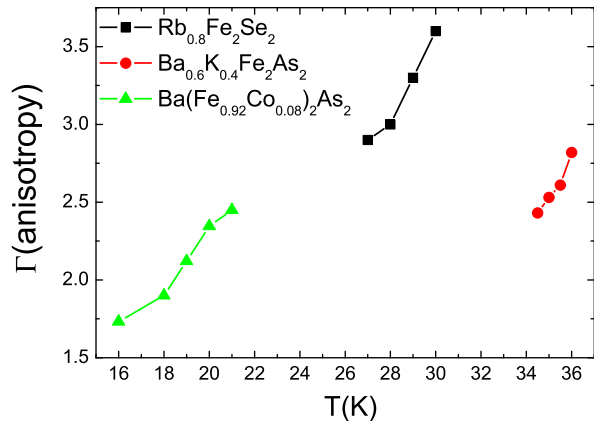


FIG. 6: The comparison of anisotropies determined for the $\text{Rb}_{0.8}\text{Fe}_2\text{Se}_2$, $\text{Ba}_{0.6}\text{K}_{0.4}\text{Fe}_2\text{As}_2$ and $\text{Ba}(\text{Fe}_{0.92}\text{Co}_{0.08})_2\text{As}_2$ single crystals.

$\text{Ba}_{0.6}\text{K}_{0.4}\text{Fe}_2\text{As}_2$ and $\text{Ba}(\text{Fe}_{0.92}\text{Co}_{0.08})_2\text{As}_2$ single crystals are shown in Fig. 6. It is found that, the anisotropy of $\text{Rb}_{0.8}\text{Fe}_2\text{Se}_2$ decreases slightly with decreasing temperature. This kind of temperature dependence of $\Gamma(T)$ is consistent with other FeAs-122 superconductors, such as $\text{Ba}_{0.6}\text{K}_{0.4}\text{Fe}_2\text{As}_2$, $\text{Ba}(\text{Fe}_{0.92}\text{Co}_{0.08})_2\text{As}_2$, etc.. This may be understood as the multiband effect, or the effect due to gradual setting in of the pair breaking by the spin-paramagnetic effect which requires $H_{c2}^{ab} = H_{c2}^c$ in the high field limit. It should be noted that the good scaling behavior suggests a field-independent anisotropy in the temperature and field range we investigated.²³ Compared to MgB_2 and cuprate superconductor, anisotropy of $\text{Rb}_{0.8}\text{Fe}_2\text{Se}_2$ is very small and lower than that of FeAs-

1111 family such as $\text{NdFeAsO}_{1-x}\text{F}_x$, while it is little higher than that in hole and electron doped FeAs-122 superconductors and similar to that of KFe_2As_2 with the same structure. It is however very strange that KFe_2As_2 and $\text{K}_x\text{Fe}_2\text{Se}_2$ should reside in the two terminals of the phase diagram, the former is strongly hole doped, while the latter is electron doped. The larger anisotropy in $\text{K}_x\text{Fe}_2\text{Se}_2$ may suggest a more two dimensional Fermi surface in this material. So far no angle resolved photo-emission spectroscopy (ARPES) on the $\text{A}_x\text{Fe}_2\text{Se}_2$ family has been reported. The difference between the anisotropy in $\text{Ba}_{0.6}\text{K}_{0.4}\text{Fe}_2\text{As}_2$ and $\text{Rb}_{0.8}\text{Fe}_2\text{Se}_2$ may hinge on that the latter has less warped Fermi surface. Our results here should be stimulating in fulfilling a quantitative calculation and further studying on the electronic structure of this new family, and ultimately providing an understanding to the underlying mechanism of superconductivity.

In conclusion, we successfully fabricate single crystals of $\text{Rb}_{0.8}\text{Fe}_2\text{Se}_2$ with the superconducting transition temperatures $T_c^{\text{onset}} = 31$ K. A clear anomaly of the resistivity was observed in the normal state at about 150 K. We also determined the upper critical fields along ab-plane and c-axis. The anisotropy of the superconductor determined by the ratio of H_{c2}^{ab} and H_{c2}^c is estimated to 3.5. The angle dependent resistivity measured below T_c allow a perfect scaling based on the anisotropic Ginzburg-Landau theory. The consistent value of the anisotropy is acquired which decreases from about 3.6 at 30 K around T_c to 2.9 at 27 K. Comparing to the anisotropy determined for $\text{Ba}_{0.6}\text{K}_{0.4}\text{Fe}_2\text{As}_2$ and $\text{BaFe}_{1.92}\text{Co}_{0.08}\text{As}_2$ using the same method, we expect that the Fermi surfaces in the new system $\text{A}_x\text{Fe}_2\text{Se}_2$ is less warped.

This work is supported by the Natural Science Foundation of China, the Ministry of Science and Technology of China (973 project No: 2011CBA00102), and Chinese Academy of Sciences.

-
- ¹ Y. Kamihara, T. Watanabe, M. Hirano, and H. Hosono, J. Am. Chem. Soc. **130**, 3296 (2008).
 - ² M. Rotter, M. Tegel, and D. Johrendt, Phys. Rev. Lett. **101**, 107006 (2008).
 - ³ N. Ni, S. L. Bud'ko, A. Kreyssig, S. Nandi, G. E. Rustan, A. I. Goldman, S. Gupta, J. D. Corbett, A. Kracher, P. C. Canfield, Phys. Rev. B **78**, 014507 (2008).
 - ⁴ K. Sasmal et al., Phys. Rev. Lett. **101**, 107007 (2008).
 - ⁵ A. S. Sefat, R. Jin, M. A. McGuire, B. C. Sales, D. J. Singh, and D. Mandrus, Phys. Rev. Lett. **101**, 117004 (2008).
 - ⁶ J. H. Chu, J. G. Analytis, C. Kucharczyk and I. R. Fisher, Phys. Rev. B **79**, 014506 (2009).
 - ⁷ X. C. Wang, Q. Q. Liu, Y. X. Lv, W. B. Gao, L. X. Yang, R. C. Yu, F. Y. Li, and C. Q. Jin, Solid State Communications. **148**, 538 (2008).
 - ⁸ Joshua H. Tapp, Zhongjia Tang, Bing Lv, Kalyan Sasmal, Bernd Lorenz, Paul C.W. Chu, and Arnold M. Guloy, Phys. Rev. B **78**, 060505(R) (2008).
 - ⁹ Michael J. Pitcher, Dinah R. Parker, Paul Adamson, Sebastian J. C. Herkelrath, Andrew T. Boothroyd, and Simon J. Clarke, Chem. Commun. **45**, 5918-20 (2008).
 - ¹⁰ X. Y. Zhu, F. Han, G. Mu, P. Cheng, B. Shen, B. Zeng, and H. H. Wen, Phys. Rev. B **79**, 220512(R) (2009).
 - ¹¹ Fong-Chi Hsu, Jiu-Yong Luo, Kuo-Wei Yeh, Ta-Kun Chen, Tzu-Wen Huang, Phillip M. Wu, Yong-Chi Lee, Yi-Lin Huang, Yan-Yi Chu, Der-Chung Yan, and Maw-Kuen Wu, Proc. Natl. Acad. Sci. **105**, 14262-4 (2008).
 - ¹² S. Margadonna, Y. Takabayashi, Y. Ohishi, Y. Mizuguchi, Y. Takano, T. Kagayama, T. Nakagawa, M. Takata, and K. Prassides, Phys. Rev. B **80**, 064506 (2009).
 - ¹³ L. Zhang, D. J. Singh, and M. H. Du, Phys. Rev. B **79**, 012506 (2009).
 - ¹⁴ A. Tamai, A. Y. Ganin, E. Rozbicki, J. Bacsá, W. Meevasana, P. D. C. King, M. Caffio, R. Schaub, S. Margadonna, K. Prassides, M. J. Rosseinsky, and F. Baumberger, Phys. Rev. Lett. **104**, 104097002 (2010).
 - ¹⁵ J. Guo, S. Jin, G. Wang, S. Wang, K. Zhu, T. Zhou, M. He, and X. Chen, Phys. Rev. B **82**, 180520(R) (2010).

- ¹⁶ Y. Mizuguchi, H. Takeya, Y. Kawasaki, T. Ozaki, S. Tsuda, T. Yamaguchi, Y. Takano, arXiv:Condmat/1012.4950.
- ¹⁷ A. Krzton-Maziopa, Z. Shermadini, E. Pomjakushina, V. Pomjakushin, M. Bendele, A. Amato, R. Khasanov, H. Luetkens, and K. Conder, arXiv:Condmat/1012.3637.
- ¹⁸ M. H. Fang, H. D. Wang, C. H. Dong, Z. J. Li, C. M. Feng, J. Chen, H. Q. Yuan. arXiv:Condmat/1012.5236.
- ¹⁹ F. C. Hsu, J. Y. Luo, K. W. Yeh, T. K. Chen, T. W. Huang, P. M. Wu, Y. C. Lee, Y. L. Huang, Y. Y. Chu, D. C. Yan, and M. K. Wu, Proc. Natl. Acad. Sci. U.S.A. **105**, 14262 (2008).
- ²⁰ N. R. Werthamer, E. Helfand and P. C. Hohenberg, Phys. Rev. **147**, 295(1966).
- ²¹ W. E. Lawrence and S. Doniach, in E. Kanda (ed.) Proc. 12th Int. Conf. Low Temp. Phys. (Kyoto, 1970; Keigaku, Tokyo, 1971), P. 361.
- ²² G. Blatter, V. B. Geshkenbein, and A. I. Larkin, Phys. Rev. Lett. **68**, 875 (1992).
- ²³ Z. S. Wang, H. Q. Luo, C. Ren and H. H. Wen, Phys. Rev. B **78**, 140501(R)(2008)